Journal of NeuroVirology, 15: 371–379, 2009

ISSN 1355-0284 print / 1538-2443 online
DOI: 10.3109/13550280903214091

informa
healthcare

Transgene expression in the mouse cerebellar Purkinje cells with a minimal level of integration using long terminal repeat–modified lentiviral vectors

Kiyohiko Takayama, and Takashi Torashima

Department of Neurophysiology, Gunma University Graduate School of Medicine, Maebashi, Gunma, Japan

Lentiviral vectors (LVs), which preferentially target nondividing cells, such as neurons, are promising tools for gene therapy. However, these vectors are still unsuitable as they result in insertional mutagenesis. It is therefore essential to prevent insertional mutagenesis if these vectors are to be adopted for safe next-generation clinical applications. In order to establish safe genetic therapy with LVs, we focused on the integrase recognition sequence (att) in the long terminal repeat (LTR), which is localized at the edge of the preintegrated viral DNA. We generated LTR-modified LVs (LMLVs), by altering the conserved sequences located just before the cleavage site; this alteration prevented the integration of viral DNA into the host genome. In this study, the LMLVs significantly decreased the LV-mediated transgene expression in HeLa cells compared to the control, i.e., wild-type LTR LVs; this supposedly occurred because integration was prevented. In addition, LMLVs exhibited gene expression *in vivo* when they were injected into the mouse cerebellum. Moreover, quantitative Alu element–mediated polymerase chain reaction (Alu-PCR), which detects integrated viral DNA, revealed that rate of LMLV-suppressed integration was approximately 1/500-fold compared to that in the case of the wild-type LTR LV. These data suggest that LMLVs efficiently prevent integration as well as exhibit LV-mediated gene expression in mouse cerebellar Purkinje cells *in vivo*. *Journal of NeuroVirology* (2009) **15**, 371–379.

Keywords: lentiviral vectors; insertional mutagenesis; Purkinje cells; NILVs; viral integration; integrase mutant; Alu-PCR

Introduction

Gene therapy shows great promise and potential in the treatment of diseases with no known medical treatment, as well as incurable diseases. Gene transfer strategies using viral or nonviral vectors have been employed in clinical applications; however, most of these strategies are still not up to the mark in terms of reliability and safety (Verma and Somia, 1997). Therefore, improvement of these methods is essential to establish next-generation gene therapy. Lentiviral vectors (LVs) are promising tools for transduction of nondividing cells such as neurons (Torashima *et al*, 2006a; Wong *et al*, 2004), liver cells (Follenzi *et al*, 2004), retinal cells (Yanez-Munoz *et al*, 2006), and other somatic cells (Apolonia *et al*, 2007; Lu *et al*, 2005).

Lentiviruses were originally categorized into the *Retroviridae* family, whose members have the ability to replicate within an infected cell; this family includes the leukemia and acquired immunodeficiency syndrome (AIDS) viruses. This replication ability of lentiviruses should be eliminated if they are to be employed as viral vectors for gene therapy. To eliminate the risk of employing a replication-competent virus during vector production, the viral

Address correspondence to Takashi Torashima, Department of Neurophysiology, Gunma University Graduate School of Medicine, Maebashi, Gunma, 371-8511, Japan. E-mail: ttorashima@gmail.com

The LV-producing plasmid and MSCV promoter were kindly provided by the St. Jude Children's Research Hospital and American National Red Cross, respectively. The authors thank Ms. Chiho Koyama and Ms. Yumiko Iwazaki for their technical assistance. This work was supported by a Grant-in-Aid for Scientific Research from Takeda Science Foundation (to T. T.) and Japan Intractable Diseases Research Foundation (to T. T.). The authors declare that they have no competing financial interests.

Received 18 March 2009; revised 16 April 2009; accepted 23 July 2009.

genome was categorized as follows: structural protein sequences, regulatory protein sequences, envelope proteins, and plasmid sequences containing the gene of interest (Ailles and Naldini, 2002; Naldini *et al*, 1996). Previous studies have demonstrated the elimination of all accessory genes from the packaging plasmid (Kim *et al*, 1998; Reiser *et al*, 1996; Zufferey *et al*, 1997). The lentiviral LTR contains three domains, namely, U3, R, and U5. Deletion of the promoter and enhancer sequences from the 3′ long terminal repeat (LTR) or removal of the transcriptional elements located on the U3 LTR results in the inactivation of proviral LTR, generating self-inactivating LVs (SILVs) (Iwakuma *et al*, 1999; Miyoshi *et al*, 1998; Schnell *et al*, 2000; Zufferey *et al*, 1998).

Nevertheless, recent study has identified the use of LVs as a risk factor although they are SILVs (Bokhoven *et al*, 2009). This risk was due to the activation of a protooncogene near the insertion site of the viral genome or interruption and inactivation of important genes due to vector insertion, i.e., insertional mutagenesis (Ailles and Naldini, 2002; Hanawa *et al*, 2005). Integration may lead to tumors, including leukemia or lymphoma, due to the up-regulation of cellular oncogenes (Hacein-Bey-Abina *et al*, 2003; Woods *et al*, 2006). Therefore, for clinical application of these vectors, it is essential to generate safe SILVs expressing sufficient levels of the transgene as well as minimize the risk of insertional mutagenesis. Tactical methods for producing nonintegrating LVs (NILVs) that target viral integrase and the integration process have been reported. A previous study reported the generation of D64V or E152A mutants, which are effective integrase mutants. These mutants produce activity-deficient integrase due to a mutation of one or a few amino acid(s) in the catalytic domain of integrase (Leavitt *et al*, 1996). These vectors were used to infect the mouse retina and brain (Yanez-Munoz *et al*, 2006) and mouse central nervous system (Rahim *et al*, 2009), and they were adopted for NILV-related tumor therapy (Karwacz *et al*, 2009). There are other methods to generate NILVs besides the generation of an integrase mutant; these involve alteration of the conserved sequences of att in viral LTR (Masuda *et al*, 1998; Sherman *et al*, 1992). Here, we generated att-mutant–related, LTR-modified LVs (LMLVs) and examined their properties by infecting the mouse cerebellum and quantifying the level of integration as compared to that of wild-type LTR LV by Alu element–mediated polymerase chain reaction (Alu-PCR). These data will verify the safety and the value of LMLVs for clinical applications.

Results

Generation of LTR-modified constructs for producing the lentiviral vector

We generated three types of LMLVs, namely, the U5 mutant, U3 mutant, and a U5/U3 double mutant, expressing green fluorescent protein (GFP) (Figure 1A). The bases in the conserved sequences (CA) were replaced with other bases (TG) to generate a deficient LTR-type strain. The details of the mutation are shown in Figure 1B. Each LTR mutant fragment was switched and subcloned into a lentiviral generating plasmid, namely, pCL20c MSCV-GFP, which is a GFP-expressing plasmid driven by a murine stem cell virus (MSCV) promoter.

Quantitative differences in the amounts of LTR-modified virions and wild-type virions

We visualized virion particles derived from the U5 mutant, U3 mutant, double-mutant, and wild-type LTR lentiviruses using antibodies against the viral envelope protein, namely, the vesicular stomatitis virus G protein (VSV-G) by Western blot analysis. The total amount of chemiluminescence from each virion derived from the LTR mutants was nearly equal to that in the case of the wild-type LTR lentiviral virion even though the LTR was modified (Figure 2A). Statistical data also showed that there

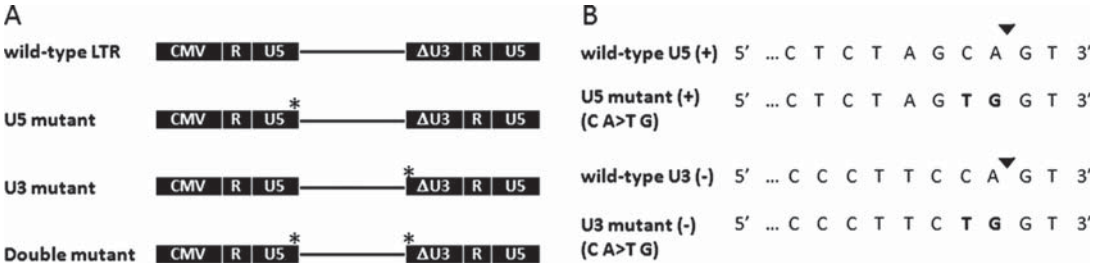

Figure 1 The mutated sites of the U5 and U3 mutants in the LTR of the LV-producing plasmid. (**A**) Schematic diagram of LTR-modified constructs for generating LMLVs. The conserved sequences (CA) were located in 3′ U5 or 5′ deleted-U3 in the LTR. Genomic RNA is packed between the 5′ R and 3′ R into virions. After viral infection, preintegrated DNA will be synthesized from genomic RNA as a template. Preintegrated DNA has 5′ U3 and 3′ U5, and both conserved sequences (CA) are strategically located and automatically mutated. (**B**) Detailed sequences of LTR modification. Each mutant was generated by switching the bases in the conserved sequences (CA) to TG bases. Asterisks indicate the mutated position in the LTR. Triangles indicate the cleavage site in the LTR. Lines indicate the sequences of the promoter and gene of interest between LTR-LTR. Bold letters show the position of the mutation. (+) and (−) indicate the sense and antisense strands, respectively.

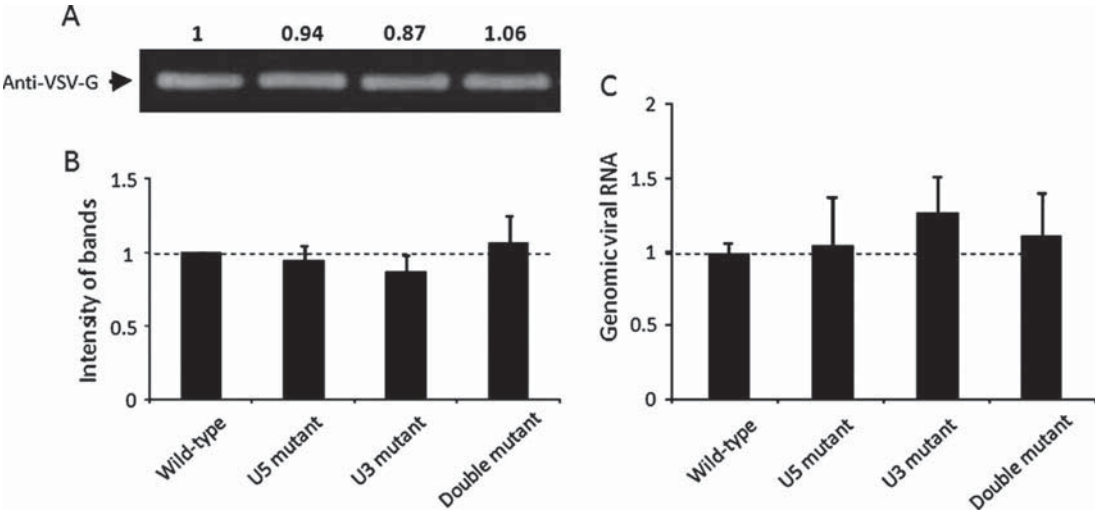

Figure 2 Quantification of lentiviruses produced from LMLVs. (**A**) An equal volume of viral solution derived from wild-type, U5 mutant, U3 mutant, and double-mutant lentiviruses were visualized with the antibody against the viral envelope protein, namely, the vesicular stomatitis virus G protein. (**B**) A quantitative Western blot analysis was obtained in the case of the wild-type lentivirus and each LMLV. Digital scores were calculated from four independent samples and indicated the mean relative amount of viral virions, respectively. (**C**) Genomic quantitative RT-PCR using an equal volume of viral solution derived from wild-type or each mutant. Data were obtained from five independent samples, respectively.

are no significant quantitative differences between the mutant LTR- and wild-type LTR lentiviral virions (Figure 2B). We next performed another method for titration of lentiviruses derived from the wild-type and mutants by genomic quantitative reverse transcriptase–polymerase chain reaction (RT-PCR). These data also revealed that there were no quantitative differences between the wild-type lentivirus and LMLVs (Figure 2C). These data indicated that LTR modification did not affect the efficiency of lentiviral production.

LMLV-mediated negligible gene expression in dividing cells (HeLa cells)

In order to examine the expression of transgenes by LMLVs in dividing cells, the lentiviruses derived from the U5 mutant, U3 mutant, double-mutant, or wild-type LTR were inoculated to a HeLa cell culture. GFP fluorescence was observed 4 days after infection; there were significantly fewer GFP-positive cells (Figure 3B, C) in the lentivirus derived from the U5 and U3 mutants. Moreover, the fluorescence intensity was also lower in these cells (Figure 3B, C) compared to the abundant GFP expression in the case of wild-type LTR LV (Figure 3A). In the case of the lentivirus derived from the double LTR mutant, it was very difficult to find GFP-positive cells, and the fluorescence was drastically faint (Figure 3D). Statistical data of the number of GFP-positive cells and the mean fluorescence intensity of the GFP-positive cells are shown in Figure 3E and F. According to our data, the number of GFP-positive cells as well as the mean fluorescence intensity of GFP-positive cells were significantly decreased in the case of the LVs derived from the U5 and U3 mutants (by approximately 40%~60%) as well as the double mutant (approximately by 90%).

Infection of LMLVs with a minimal level of integration in dividing cells (HeLa cells)

We next examined the integration of the viral genome derived from U5 mutant, U3 mutant, double-mutant, or wild-type LTR in host genome with HeLa cells. HeLa cells were collected at 4 days after lentiviral infection, and real-time quantitative Alu-PCR was performed. The results showed that the rate of integration was significantly reduced in the case of the U5 mutant (0.316 ± 0.096) and U3 mutant (0.343 ± 0.077) compared to that in the case of the wild-type LTR LV, which was adjusted to 1.0 (Figure 3G). Moreover, the integration signal in the case of the double mutant was severely reduced (0.011 ± 0.004, approximately 1/100-fold). These data suggested that LTR modification significantly prevents viral integration and this effect was further enhanced in the case of the LTR double mutant, resulting in negligible LMLV-mediated gene expression in a HeLa cell culture.

LMLVs injection in the mouse cerebellum and their transduction properties

We next examined whether LMLVs were infectious *in vivo.* In this experiment, we selected only the double mutant because it exhibited the lowest rate of integration in HeLa cells among the three LTR mutants. Consequently, the lentiviruses were injected into the mouse cerebellum. Our previous study revealed that the lentiviral vector exhibits infectious tropism toward neuronal cells, especially cerebellar Purkinje cells (Takayama *et al*,

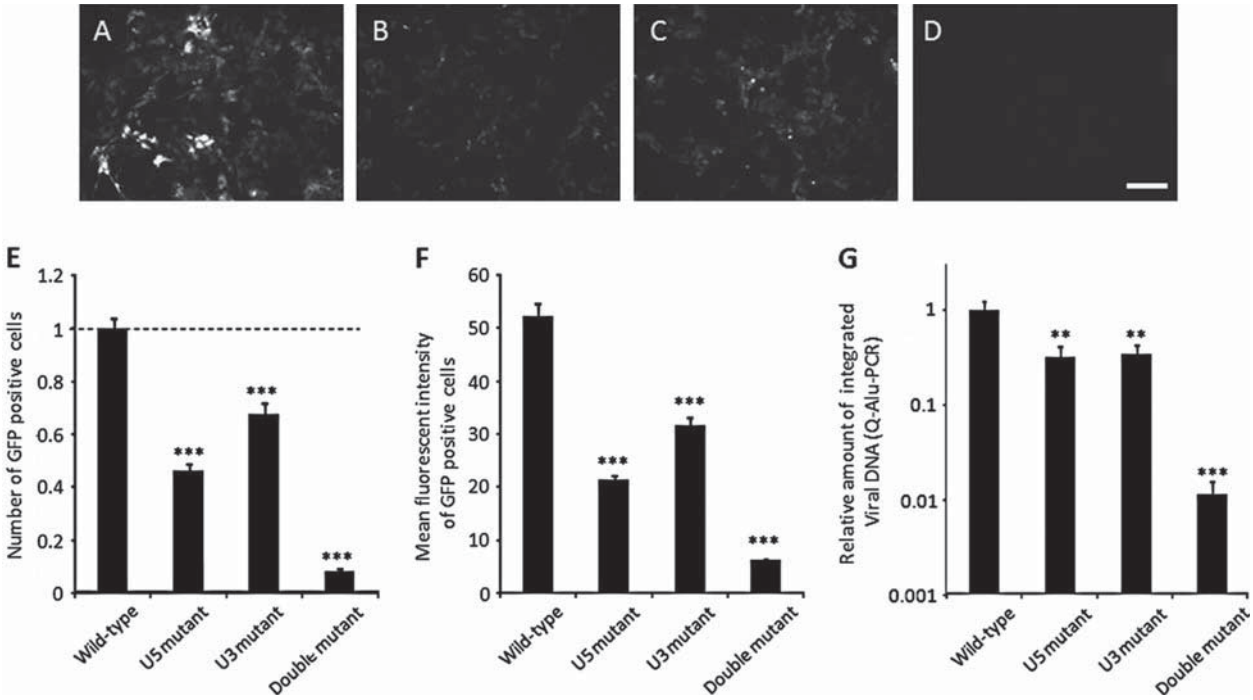

Figure 3 LTR-modification decreased LV-mediated gene expression in HeLa cells. Fluorescent images of wild-type (**A**) or LMLV-infected HeLa cells, including the U5 mutant (**B**), U3 mutant (**C**), and double mutant (**D**), detected by fluorescent microscopy 4 days after infection of the GFP-expressing lentivirus. (**E, F**) Quantitative analysis of GFP-expressing HeLa cells. A comparison of the number of GFP-positive cells between the wild-type LTR-infected HeLa cells and each LMLV-infected HeLa cells is shown in **E**. The score of the wild-type LTR was adjusted to 1.0. A comparison of the mean fluorescent intensity of GFP-positive cells between the wild-type LTR and each LMLV-infected HeLa cell is shown in **F**. (**G**) Statistical Alu-PCR analysis in order to detect integrated viral DNA in a HeLa cell genome. The rate of integration of wild-type LV or each LMLVs into the genome of the infected HeLa cells was calculated from an independent culture of the wild-type (n=8), U5 mutant (n=10), U3 mutant (n=10), and double mutant (n=9). The score of wild-type LTR was adjusted to 1.0. $^{**}P<.01$; $^{***}P<.001$. Scale bar = 20 μm.

2008; Torashima *et al*, 2006a). Mice whole brains were examined at 2 weeks after lentiviral infection by fluorescent stereomicroscopy. Widespread GFP fluorescence was detected in the cerebellum in the case of the LMLVs derived from the double mutant as well as wild-type LTR LV (Figure 4Aa, b). In addition, sagittal sections of the cerebellum showed satisfactory GFP expression similar to that in the case of wild-type LTR LV (Figure 4Ba), and lentiviral vector tropism was preserved even though the LTR was modified (Figure 4Bb). These data indicated that LMLVs derived from the double mutant exhibit transgene expression in neurons, such as the mouse cerebellar Purkinje cells, and its tropism was preserved compared to wild-type LV *in vivo.*

Safe and satisfactory gene expression using LMLVs in the mouse cerebellum

Our previous experiments revealed that LMLVs promote satisfactory gene expression in the mouse cerebellum. However, this is not of consequence if the gene expression is due to an integrated transgene. Thus, we finally examined whether the transgene derived from the LMLV was integrated into the chromosomal genome of the mouse cerebellum. We then attempted to quantify LMLVs by real-time Alu-PCR using the LMLV-injected mouse cerebellum. Surprisingly, the integration rate in the case of the double mutant–injected mouse was significantly reduced (0.002 ± 0.002, approximately 1/500-fold), compared to that in the case of the wild-type LTR LV, which was adjusted to 1.0 (Figure 5A). In addition, the total copy number of the MSCV promoter, which promoted GFP expression in Purkinje cells, was calculated. There were no quantitative differences in the total amount of GFP-expressing promoter between the wild-type lentivirus and the double mutant (Figure 5B), statistically. These data strongly revealed that LMLVs are remarkable and useful mutants that can promote satisfactory gene expression with a minimal level of integration in the mouse brain.

Discussion

LVs are promising tools for transduction of foreign genes, except for a potential problem associated with integration. Therefore, it is essential to produce NILVs for safer clinical applications. Previous studies have reported the basic properties of integrase-deficient NILVs, such as D64V or E152A mutants, using several cell lines (Leavitt *et al*, 1996). Further, their usefulness for the infection of nondividing

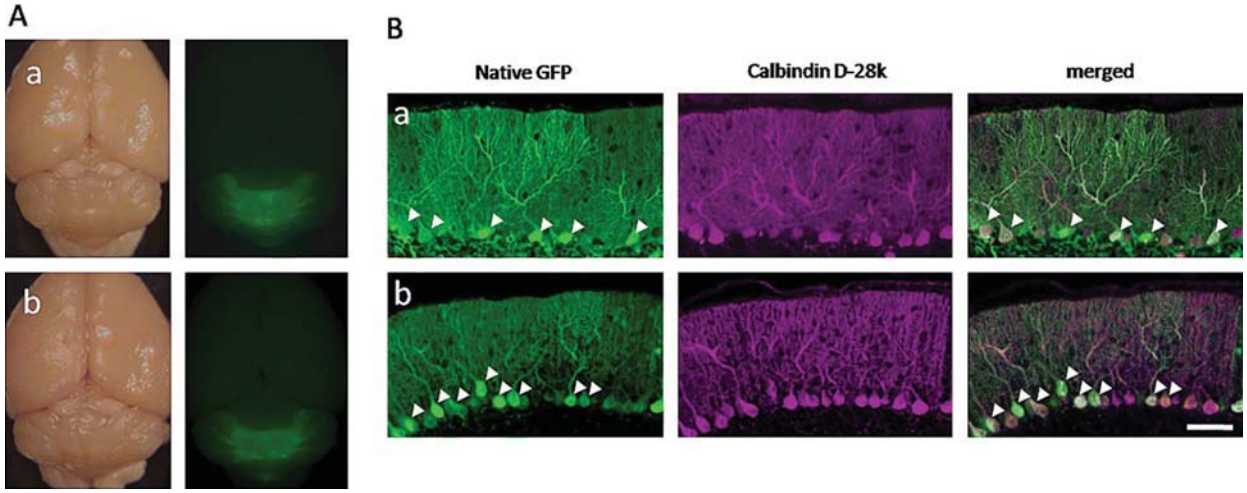

Figure 4 LVs mediated satisfactory gene expression by LTR modification in mouse cerebellar Purkinje cells. (**A**) Typical images of the mouse whole brain at 2 weeks after injection of GFP-expressing wild-type LTR lentivirus (**A**, a) and double mutant LMLV (**A**, b). Bright field (left) and fluorescent (*right*) images are shown in **A**. (**B**) Immunohistochemical staining of the LMLV-injected mouse cerebellum. Sagittal sections in which native GFP fluorescence is observed after injection with wild-type LTR lentivirus (**B**, a) or the double mutant LMLV (**B**, b) are shown (*left*). Sections were counterstained with a Purkinje cell–specific marker, calbindin D-28k (magenta), for visualizing the somata and dendrites of Purkinje cells (*middle*). The native GFP (*green*) was merged with magenta images (*right*). Triangles indicate the somata of cerebellar Purkinje cells. Scale bar = 50 μm.

cells, such as neurons (Philippe *et al*, 2006; Nightingale *et al*, 2006; Li *et al*, 2001), and *in vivo* vector-mediated gene expression in muscle cells (Apolonia *et al*, 2007) has also been reported. However, the infection properties of these virions in the brain are still unknown.

In this study, we aimed at generating safe viral vectors and produced the LTR-modified LVs (LMLVs). It has been shown that Alu-PCR and linear amplification-mediated (LAM)-PCR and are powerful methods for detecting integrated viral DNA (Brussel *et al*, 2005; Schmidt *et al*, 2007). Therefore, to clarify the safety of LMLVs, we performed real-time quantitative nested Alu-PCR using LMLV-infected samples. In this step, we only targeted integrated viral DNA and not 1-LTR or 2-LTR circularized viral DNA because we speculated that this method enabled direct detection of integrated viral DNA.

In the HeLa cell study, we were barely able to detect gene expression and viral integration when LMLVs were applied. However, these results were evidently a consequence of the failure of integration followed by cell division, and confirmed the previous data (Li *et al*, 2001). The extent of GFP-labeled area in the mouse cerebellum varied to some extent with every viral injection, although the same batch of

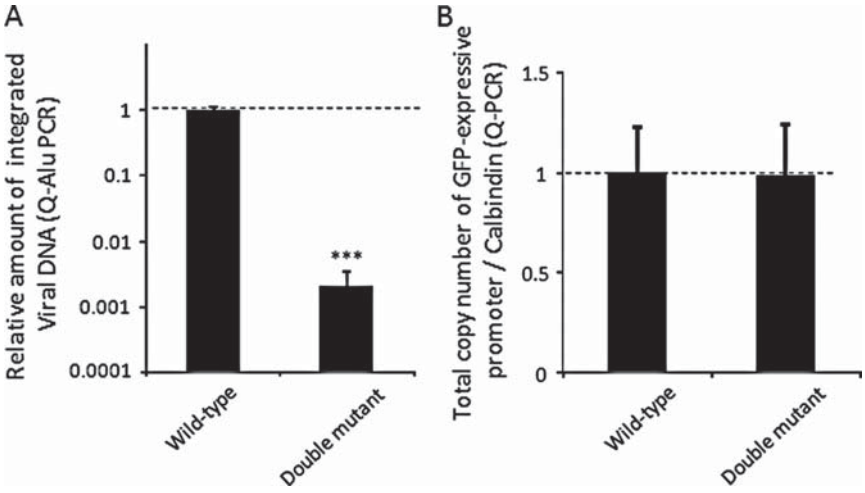

Figure 5 Quantitative analysis of the LMLV-injected mouse cerebellum at 2 weeks after injection. (**A**) Alu-PCR to detect the integrated transgene in the viral-injected cerebellum. (**B**) Quantification of the total copy number of the GFP-expressing promoter. The integration rate in the case of the wild-type LV– or double-mutant LMLV–infected cerebellum were calculated in the case of mice that were injected with wild-type LV (n=4) or the double mutant (n=4). The score of wild-type LTR was adjusted to 1.0. Data were conducted in three replicates for each sample, respectively. ***P<.001.

virus was injected. However, the expression level of the well-infected area was almost constant in the case of every injection (data not shown). In contrast with the results of the *in vitro* study, the *in vivo* experiment using cerebellar Purkinje cells, which are the output neurons in the cerebellum, revealed that there was satisfactory transgene expression with a minimal level of viral integration when LMLVs were applied. In addition, MSCV-driven GFP expression was highly restricted to Purkinje cells (Torashima *et al*, 2006b). This tropism was preserved in the NILVs application trial. These data strongly suggest that LMLVs are suitable tools for safe transduction of nondividing cells such as neurons.

From a therapeutic viewpoint, long-lasting gene expression and residual background integration of LMLVs are other important subjects to be considered. These issues have been clarified by inoculating integrase-deficient NILVs into mouse tissues. Yanez-Munoz *et al* revealed that NILV-mediated gene expression was prolonged up to 9 months in mouse ocular tissues. In addition, Apolonia *et al* showed that integrase-deficient NILVs have significantly less residual background integration as compared with att-mutant NILVs. Therefore, in this study, we only focused on the properties of LMLVs with respect to the integration process and prevention of insertional mutagenesis, and did not examine sustained gene expression or compare our vector with integrase-deficient NILVs.

The NILV development strategy was aimed at safe clinical applications. Some groups succeeded in achieving efficient gene delivery *in vivo* using NILVs (Apolonia *et al*, 2007; Rahim *et al*, 2009; Yanez-Munoz *et al*, 2006) or NILV-related gene therapy (Karwacz *et al*, 2009). In this study, we generated att-mutant–related NILVs, which are LMLVs, but not integrase-mutant–related NILVs, and verified the safety of these vectors using Alu-PCR as well as certified the usefulness of LMLVs in the mouse cerebellar Purkinje cells. We hope that this report will contribute in a big way toward NILV gene therapy and clinical applications of NILVs in future.

Materials and methods

Animals

Six week-old C57BL/6J mice were obtained from Japan SLC (Shizuoka, Japan) for viral injection. All procedures for the care and treatment of animals were carried out according to the National Institutes of Health (NIH) guidelines, and the experimental protocol was approved by the institutional committee of Gunma University.

Preparation of LTR-modified constructs

LTR-modified constructs, the U5 mutant and U3 mutant, were generated by a two-step PCR using the original LV-producing plasmid, pCL20c-MCSV-GFP (kindly provided by Dr. Nienhuis). The detailed mutation position of U5 and U3 are described in Figure 1. The former or later fragment of the U5 mutant was extended with U5 Pvu-S, 5′-CCT CCG ATC GTT GTC AGA AG-3′ and U5 mut-A, 5′-GGG CGC CAC **CA**C TAG AGA TTT TCC ACA CTG AC-3′ or U5 mut-S, 5′-AAT CTC TAG **TG**G TGG CGC CCG AAC AGG G-3′ and U5 Mfe-A, 5′-TCT CCA ATT GTC CCT CAT ATC T-3′, respectively. The former or later fragment of the U3 mutant was extended with U3 Eco-S, 5′-GGA ATT CTG CAG TCG ACG GT-3′ and U3 mut-A, 5′-AGC CCT TC**T G**GT CCC CCC TTT TCT TTT AAA AA-3′ or U3 mut-S, 5′-GGG GGG AC**C A**GA AGG GCT AAT TCA CTC CCA-3′ and U3 Xho-A, 5′-CTA GCT CGA GCA GCT GAA G-3′, respectively (bold letters indicate mutation position in each primer set). The mutated second PCR fragments between former and later were placed in the same position as that of the wild-type LV plasmid. A double mutant was generated from the U5 mutant by the same procedure used for generating the U3 mutant. The presence of the desired mutations was confirmed by DNA sequencing using primers that were designed 100 to 110 bp upstream from the mutation (U5-check, 5′-TAG GGA ACC CAC TGC TTA AG-3′; U3-check; 5′-CGG CAT GGA CGA GCT GTA C-3′).

Preparation of LMLVs

Vesicular stomatitis virus G protein (VSV-G)–pseudotyped HIV vectors were used in this study. The backbones of helper plasmids were derived from pCAGGS (Niwa *et al*, 1991). The viral vectors were designed to express the GFP protein with wild-type LV or modified LTR LV under the control of the murine stem cell virus (MSCV) ubiquitous promoter (Hawley *et al*, 1994). The detailed procedure for viral vector production was described in a previous report (Torashima *et al*, 2006a). Briefly, viral vectors were produced from human embryonic kidney (HEK) 293 T cells, which were maintained in Dulbecco's modified Eagle's medium (DMEM) containing 10% fetal bovine serum (FBS), by cotransfection of four plasmids, namely, pCL20cMSCV-GFP, pCAGkGP1R, pCAG4RTR2, and pCAGVSV-G, by a calcium phosphate precipitation method. After transfection, the cells were cultured for 16 h; thereafter, they were washed and cultured for an additional 24 h. The LV-containing medium was harvested and centrifuged at 25,000 rpm for 90 min followed by filtration through 0.22-μm membranes. Viral pellets were finally resuspended in 70 μl phosphate buffered saline (PBS; pH 7.4) and stored at 4°C.

Western blot

The procedure of Western blot has been described previously (Matsuda *et al*, 1999). Briefly, 1 μl of lentivirus derived from the wild-type, U5 mutant,

U3 mutant, and double mutant were solubilized directly in 99 µl of 1 × sample buffer and denatured at 95°C for 5 min. Subsequently, samples were electrophoresed on 10% sodium dodecyl sulfate (SDS) polyacrylamide gels and transferred onto polyvinylidene difluoride (PVDF) membranes. Blots were incubated with rabbit polyclonal anti-VSV-G antibodies (1:10,000; Sigma, St. Louis, MO, USA) followed by the incubation of horseradish peroxidase (HRP)-conjugated secondary antibody. The relative amount of immunoreactive VSV-G band in each lane was quantified using an image analyzer (Basic Quantifier; Japan Bio Image) during each Western blot run. The viral amount was normalized by the intensity of virions (based on wild-type LTR lentivirus at 1×10^{10} TU/ml) for infection to HeLa cells or injection into mouse cerebellum. Statistical graphs were prepared from four independent virus preparations.

Quantitative RT-PCR

Genomic RNA of lentiviruses was quantified by quantitative RT-PCR procedure in which reverse transcription (RT) could be performed in the same reaction tube. The detailed procedure has been described previously (Geraerts *et al*, 2006). Briefly, after RNA extraction of the wild-type lentivirus or LMLVs with the RNA isolation kit (RNeasy Mini kit; Qiagen, Germany), a DNase was used to eliminate residual plasmid DNA. Genomic viral RNA was inverted by the primer (Lenti-RT, 5′-GGG AGT GAA TTA GCC CTT CC-3′) located in the LTR. Subsequently, quantitative PCR was carried out using the primers (forward, 5′-CAC TCC CTT AAG TTT GAC CTT-3′ and reverse, 5′-GCC AAG GCT TCC CAG GTC-3′) with the real-time thermal cycler (Thermal Cycler Dice, TP800; TaKaRa).

Viral infection of HeLa cells and fluorescence analysis

HeLa cells were seeded on a 12-well plastic plate at a density of 1×10^4 cells along with 0.1 µl of virion-related normalized lentiviruses and 1 µl (final concentration [f.c.], 6 µg/ml) of polybrene. Fluorescent images of GFP-expressing HeLa cells were obtained by fluorescent microscopy (CTR6000; Leica, Germany) 4 days after addition of lentiviruses. The total number of GFP-positive cells was counted in four different fields under the 10 × objective. The GFP fluorescence intensity was calculated from a total of 60 GFP-positive cells per construct with a data analyzing software (IPLab ver. 3.5.5; BD Bioscience, MD, USA).

Viral injection into mouse cerebellum

The detailed procedure for viral vector injection has been described in a previous report (Torashima *et al*, 2006a). Briefly, before the viral injection, C57BL/6J mice were anesthetized by 2% isoflurane (flow speed, 1 L/min) inhalation. The mouse was mounted on a stereotactic frame and the LV injected (1.0 mm, depth) with a hamilton syringe attached to a micropump (UltramicroPump II; World Precision Instruments [WPI], Sarasota, FL, USA), controlled by a microprocessor-based controller (Micro4; WPI). A burr hole was drilled on the surface of the cerebellar vermis that was located 5 to 6 mm caudal from the bregma. Six microliters of virion-related normalized LVs was injected at 300 nl/min.

Immunohistochemistry

Mice were transcardially perfused with 4% paraformaldehyde in phosphate buffer after they were anesthetized with sodium pentbarbital. The cerebellum was removed and photographs of the whole brain were obtained by fluorescent stereomicroscopy (VB-G25; Keyence, Osaka, Japan). The brains were then postfixed in the same fixative for 24 h. For immunostaining, the cerebellum was cut into 50-µm sagittal sections using a microslicer (DTK-1000; DOSAKA, Kyoto, Japan). Floating sections were immunostained with mouse monoclonal anti-calbindin D-28K (1:500; Swant, Bellinzona, Switzerland) and visualized with Alexa fluor 468-conjugated anti-mouse immunoglobulin G (IgG) (1:1,000; Invitrogen, Carlsbad, CA, USA). Fluorescent images of cerebellar slices were obtained using a confocal laser-scanning microscope (LSM 5 PASCAL; Zeiss, Oberkochen, Germany).

Quantitative Alu-PCR

First, to purify the chromosomal DNA, HeLa cells were seeded on a 5-cm culture dish at a density of 1×10^5 cells along with 1 µl of virion-related normalized LV and 5 µl (final concentration [f.c.], 6 µg/ml) of polybrene. Four days later, the HeLa cells were collected with a plastic scraper after washing with ice-cold PBS; mice were injected with the lentivirus as an *in vivo* experiment. At 2 weeks after viral injection, the mice were sacrificed and trimmed the GFP-expressing area in the cerebellum. Chromosomal DNA was purified using the genomic DNA purification kit (Promega, WI, USA) and finally eluted with 50 µl of double-distilled H_2O (ddH_2O). The details of the Alu-PCR procedure have been described in a previous report (Brussel *et al*, 2005). In short, the integrated transgene was detected by nested Alu-PCR. To avoid amplification of the nonintegrated transgene derived from the LV as well as 1-LTR or 2-LTR circular DNA, an initial PCR was carried out using an artificial sequence-tagged primer (L-M667, 5′-ATG CCA CGT AAG CGA AAC TCT GGC TAA CTA GGG AAC CCA CTG-3′) as a forward and reverse primer that targeted internal Alu sequences (Alu1, 5′-TCC CAG CTA CTG GGG AGG CTG AGG-3′; Alu2, 5′-GCC TCC CAA AGT GCT GGG ATT ACA G-3′). The reactions were performed using PrimeStar Max (TaKaRa, Shiga, Japan) with the addition of three other primers, namely, L-M667,

Alu1, and Alu2 (f.c., 10 pM each) in 20 µl of reaction volume. The thermal cycler (Mastercycler ep Gradient S; Eppendorf, Hamburg, Germany) was programmed to perform a hot start at 98°C for 5 min, followed by 35 cycles of the following: denaturation at 98°C for 10 s, annealing at 60°C for 5 s, and extension at 72°C for 2 min. The second real-time quantitative PCR was performed using 2 µl of the first PCR product. The reactions were performed using SYBR Premix EX Taq II (TaKaRa) with the addition of two nested primers (f.c., 10 pM each; namely, LambdaT, 5′-ATG CCA CGT AAG CGA AAC T-3′ and AA55M, 5′-GCT AGA GAT TTT CCA CAC TGA CTA A-3′) in 25 µl of reaction volume. The real-time PCR (Thermal Cycler Dice, TP800; TaKaRa) program began with a hot start at 95°C for 10 s, followed by 40 cycles of the following: denaturation at 95°C for 5 s and data collection at 60°C for 30 s. As a control, the primers for HeLa cells (MA050371-F, 5′-TGT GTC CGT CGT GGA TCT GA-3′ and MA050371-R, 5′-TTG CTG TTG AAG TCG CAG GAG-3′), or mouse cerebellum (MSCV-S, 5′-CAC TCC CTT AAG TTT GAC CTT-3′ and MSCV-A, 5′-GCC AAG GCT TCC CAG GTC-3′) were used for normalization during quantitative Alu-PCR.

Quantification of the total copy number of the GFP-expressing promoter

At 2 weeks after viral injection, the mice were sacrificed and the GFP-expressing area in the cerebellum was trimmed to quantify the viral copy number. The total copy number of the MSCV promoter, which promotes GFP expression in Purkinje cells, was calculated with the primers (MSCV-S, 5′-CAC TCC CTT AAG TTT GAC CTT-3′ and MSCV-A, 5′-GCC AAG GCT TCC CAG GTC-3′) by quantitative PCR. As a control, the primers (Calbindin-S, 5′-CTC TGA TCA CAG CCT CAC AGT T-3′ and Calbindin-A, 5′-GCA GAA GCT CCT GGA TCA AGT T-3′) were used for normalization during quantitative Alu-PCR. The detailed procedure has been described previously (Rahim *et al*, 2009).

Statistics

Statistical differences were analyzed by Tukey's post hoc test after one-way analysis of variance (ANOVA). Data are expressed as the mean ± SEM, unless otherwise specified.

Declaration of interest: The authors report no conflicts of interest. The authors alone are responsible for the content and writing of the paper.

References

Ailles LE, Naldini L (2002). HIV-1-derived lentiviral vectors. *Curr Top Microbiol Immunol* **261:** 31–52.

Apolonia L, Waddington SN, Fernandes C, Ward NJ, Bouma G, Blundell MP, Thrasher AJ, Collins MK, Philpott NJ (2007). Stable gene transfer to muscle using non-integrating lentiviral vectors. *Mol Ther* **15:** 1947–1954.

Bokhoven M, Stephen SL, Knight S, Gevers EF, Robinson IC, Takeuchi Y, Collins MK (2009). Insertional gene activation by lentiviral and gammaretroviral vectors. *J Virol* **83:** 283–294.

Brussel A, Delelis O, Sonigo P (2005). Alu-LTR real-time nested PCR assay for quantifying integrated HIV-1 DNA. *Methods Mol Biol* **304:** 139–154.

Follenzi A, Battaglia M, Lombardo A, Annoni A, Roncarolo MG, Naldini L (2004). Targeting lentiviral vector expression to hepatocytes limits transgene-specific immune response and establishes long-term expression of human antihemophilic factor IX in mice. *Blood* **103:** 3700–3709.

Geraerts M, Willems S, Baekelandt V, Debyser Z, Gijsbers R (2006). Comparison of lentiviral vector titration methods. *BMC Biotechnol* **6:** 34.

Hacein-Bey-Abina S, Von Kalle C, Schmidt M, McCormack MP, Wulffraat N, Leboulch P, Lim A, Osborne CS, Pawliuk R, Morillon E, Sorensen R, Forster A, Fraser P, Cohen JI, de Saint Basile G, Alexander I, Wintergerst U, Frebourg T, Aurias A, Stoppa-Lyonnet D, Romana S, Radford-Weiss I, Gross F, Valensi F, Delabesse E, Macintyre E, Sigaux F, Soulier J, Leiva LE, Wissler M, Prinz C, Rabbitts TH, Le Deist F, Fischer A, Cavazzana-Calvo M (2003). LMO2-associated clonal T cell proliferation in two patients after gene therapy for SCID-X1. *Science* **302:** 415–419.

Hanawa H, Persons DA, Nienhuis AW (2005). Mobilization and mechanism of transcription of integrated self-inactivating lentiviral vectors. *J Virol* **79:** 8410–8421.

Hawley RG, Lieu FH, Fong AZ, Hawley TS (1994). Versatile retroviral vectors for potential use in gene therapy. *Gene Ther* **1:** 136–138.

Iwakuma T, Cui Y, Chang LJ (1999). Self-inactivating lentiviral vectors with U3 and U5 modifications. *Virology* **261:** 120–132.

Karwacz K, Mukherjee S, Apolonia L, Blundell MP, Bouma G, Escors D, Collins MK, Thrasher AJ (2009). Nonintegrating lentivector vaccines stimulate prolonged T-cell and antibody responses and are effective in tumor therapy. *J Virol* **83:** 3094–3103.

Kim VN, Mitrophanous K, Kingsman SM, Kingsman AJ (1998). Minimal requirement for a lentivirus vector based on human immunodeficiency virus type 1. *J Virol* **72:** 811–816.

Leavitt AD, Robles G, Alesandro N, Varmus HE (1996). Human immunodeficiency virus type 1 integrase mutants retain in vitro integrase activity yet fail to integrate viral DNA efficiently during infection. *J Virol* **70:** 721–728.

Li L, Olvera JM, Yoder KE, Mitchell RS, Butler SL, Lieber M, Martin SL, Bushman FD (2001). Role of the non-homologous DNA end joining pathway in

the early steps of retroviral infection. *EMBO J* **20:** 3272–3281.

Lu R, Limon A, Ghory HZ, Engelman A (2005). Genetic analyses of DNA-binding mutants in the catalytic core domain of human immunodeficiency virus type 1 integrase. *J Virol* **79:** 2493–2505.

Masuda T, Kuroda MJ, Harada S (1998). Specific and independent recognition of U3 and U5 att sites by human immunodeficiency virus type 1 integrase in vivo. *J Virol* **72:** 8396–8402.

Matsuda S, Mikawa S, Hirai H (1999). Phosphorylation of serine-880 in GluR2 by protein kinase C prevents its C terminus from binding with glutamate receptor-interacting protein. *J Neurochem* **73:** 1765–1768.

Miyoshi H, Blomer U, Takahashi M, Gage FH, Verma IM (1998). Development of a self-inactivating lentivirus vector. *J Virol* **72:** 8150–8157.

Naldini L, Blomer U, Gage FH, Trono D, Verma IM (1996). Efficient transfer, integration, and sustained long-term expression of the transgene in adult rat brains injected with a lentiviral vector. *Proc Natl Acad Sci U S A* **93:** 11382–11388.

Nightingale SJ, Hollis RP, Pepper KA, Petersen D, Yu XJ, Yang C, Bahner I, Kohn DB (2006). Transient gene expression by nonintegrating lentiviral vectors. *Mol Ther* **13:** 1121–1132.

Niwa H, Yamamura K, Miyazaki J (1991). Efficient selection for high-expression transfectants with a novel eukaryotic vector. *Gene* **108:** 193–199.

Philippe S, Sarkis C, Barkats M, Mammeri H, Ladroue C, Petit C, Mallet J, Serguera C (2006). Lentiviral vectors with a defective integrase allow efficient and sustained transgene expression in vitro and in vivo. *Proc Natl Acad Sci U S A* **103:** 17684–17689.

Rahim AA, Wong AM, Howe SJ, Buckley SM, Acosta-Saltos AD, Elston KE, Ward NJ, Philpott NJ, Cooper JD, Anderson PN, Waddington SN, Thrasher AJ, Raivich G (2009). Efficient gene delivery to the adult and fetal CNS using pseudotyped non-integrating lentiviral vectors. *Gene Ther* **16:** 509–520.

Reiser J, Harmison G, Kluepfel-Stahl S, Brady RO, Karlsson S, Schubert M (1996). Transduction of nondividing cells using pseudotyped defective high-titer HIV type 1 particles. *Proc Natl Acad Sci U S A* **93:** 15266–15271.

Schmidt M, Schwarzwaelder K, Bartholomae C, Zaoui K, Ball C, Pilz I, Braun S, Glimm H, von Kalle C (2007). High-resolution insertion-site analysis by linear amplification-mediated PCR (LAM-PCR). *Nat Methods* **4:** 1051–1057.

Schnell T, Foley P, Wirth M, Munch J, Uberla K (2000). Development of a self-inactivating, minimal lentivirus vector based on simian immunodeficiency virus. *Hum Gene Ther* **11:** 439–447.

Sherman PA, Dickson ML, Fyfe JA (1992). Human immunodeficiency virus type 1 integration protein: DNA sequence requirements for cleaving and joining reactions. *J Virol* **66:** 3593–3601.

Takayama K, Torashima T, Horiuchi H, Hirai H (2008). Purkinje-cell-preferential transduction by lentiviral vectors with the murine stem cell virus promoter. *Neurosci Lett* **443:** 7–11.

Torashima T, Okoyama S, Nishizaki T, Hirai H (2006a). In vivo transduction of murine cerebellar Purkinje cells by HIV-derived lentiviral vectors. *Brain Res* **1082:** 11–22.

Torashima T, Yamada N, Itoh M, Yamamoto A, Hirai H (2006b). Exposure of lentiviral vectors to subneutral pH shifts the tropism from Purkinje cell to Bergmann glia. *Eur J Neurosci* **24:** 371–380.

Verma IM, Somia N (1997). Gene therapy – promises, problems and prospects. *Nature* **389:** 239–242.

Wong LF, Azzouz M, Walmsley LE, Askham Z, Wilkes FJ, Mitrophanous KA, Kingsman SM, Mazarakis ND (2004). Transduction patterns of pseudotyped lentiviral vectors in the nervous system. *Mol Ther* **9:** 101–111.

Woods NB, Bottero V, Schmidt M, von Kalle C, Verma IM (2006). Gene therapy: therapeutic gene causing lymphoma. *Nature* **440:** 1123.

Yanez-Munoz RJ, Balaggan KS, MacNeil A, Howe SJ, Schmidt M, Smith AJ, Buch P, MacLaren RE, Anderson PN, Barker SE, Duran Y, Bartholomae C, von Kalle C, Heckenlively JR, Kinnon C, Ali RR, Thrasher AJ (2006). Effective gene therapy with nonintegrating lentiviral vectors. *Nat Med* **12:** 348–353.

Zufferey R, Dull T, Mandel RJ, Bukovsky A, Quiroz D, Naldini L, Trono D (1998). Self-inactivating lentivirus vector for safe and efficient in vivo gene delivery. *J Virol* **72:** 9873–9880.

Zufferey R, Nagy D, Mandel RJ, Naldini L, Trono D (1997). Multiply attenuated lentiviral vector achieves efficient gene delivery in vivo. *Nat Biotechnol* **15:** 871–875.